Journal of Marine Research, 53, 49–77, 1995

On geostrophic adjustment of a two-layer, uniformly rotating fluid in the presence of a step escarpment

by A. J. Willmott[1] and E. R. Johnson[2]

ABSTRACT

This paper addresses the Rossby adjustment problem for an inviscid uniformly rotating two-layer fluid in the presence of a step escarpment of infinite length. The problem can be solved analytically for the case when the ratio of the step height to the average depth of the lower layer is small. In this case two well-separated adjustment time scales emerge; the rapid, inertial and the slow, topographic vortex-stretching time scales.

The fluid is assumed to be at rest initially with imposed step discontinuities in the free surface and interfacial displacements oriented perpendicular to the escarpment. A two time-scale approach shows that during the rapid inertial adjustment the fluid is not influenced by the topography. On the slow vortex-stretching time scale the fluid adjusts via the propagation of topographic Rossby waves, modified by stratification, along the step. A steady state solution is established in which the flow is geostrophically balanced in both layers. Therefore, in this steady state no fluid in the lower layer crosses the escarpment. However, cross-escarpment flow occurs in the upper layer. The volume of fluid in the upper layer that crosses the escarpment, rather than being deflected parallel to the topography, is calculated.

1. Introduction

The topology of the density surfaces and the location and strength of currents in the ocean will sometimes be a reflection of the contemporaneous forcing of the ocean through heating, evaporation, precipitation and wind stress. However during periods where forcing is weak the many ocean flows appear to relax to geostrophically adjusted states. These adjusted flows are not unique. It was the insight of C. G. Rossby that a unique solution could be obtained by considering an initial value problem. Rossby's adjusted solutions have proven invaluable in discussing flows observed in the oceans, laboratory and numerical simulations. It is the purpose of the present paper to derive similar adjusted solutions incorporating the effects of stratification and varying bottom topography. Observations of stratified adjustment in the presence of depth variations are still relatively uncommon but a comparison of

1. Department of Mathematics, University of Exeter, North Park Road, Exeter, EX4 4QE, United Kingdom.
2. Department of Mathematics, University College London, Gower Street, London, WC1E 6BT, United Kingdom.

our results with those available at present are given in a discussion at the end of the text.

The "classical" Rossby adjustment problem for a uniformly rotating homogeneous fluid (see Gill *et al.,* 1986, for an excellent review of the problem) has received renewed interest with the introduction of topography (Johnson, 1985; Gill *et al.,* 1986; Johnson and Davey, 1990; Willmott and Grimshaw, 1991; 1992). Topography supports topographic Rossby waves, whose phase propagates with shallow water to the right (in the Northern Hemisphere). This introduces an asymmetry into the evolution of flows above uneven bathymetry. For example, when fluid is forced to cross a depth discontinuity it will be diverted in the direction that double Kelvin waves propagate (Gill *et al.,* 1986).

In the ocean, escarpments are not infinitely long and terminate where they meet ocean boundaries. When fluid is confined to a semi-infinite domain by a vertical side wall with a step escarpment oriented perpendicular to the wall, Gill *et al.* (1986) obtain an analytical solution for the steady adjusted geostrophic flow. Using the same geometry, Johnson (1985) analytically solved the full initial value problem for the evolution of a flow driven by a source-sink pair located on the wall symmetrically about the step. Both Johnson (1985) and Gill *et al.* (1986) employ the rigid-lid approximation, in which case the energy propagation associated with double Kelvin waves is unidirectional; there is no reversal of group velocity for short waves. Still employing the rigid-lid approximation, Willmott and Grimshaw (1991, 1992) replace the step escarpment with a wedge-shaped escarpment, the apex of which lies on the vertical wall. Energy can now propagate in either direction along the escarpment via topographic Rossby waves. They show that long waves are again responsible for establishing the steady geostrophic flow over the wedge-shaped escarpment, when a source-sink driven flow of the type described by Johnson (1985) is impulsively switched-on and maintained. Further, in the final solution, Willmott and Grimshaw (1991) find that the fluid above the escarpment is motionless. The establishment of a steady solution in Willmott and Grimshaw (1991, 1992) is only possible because the escarpment width is zero at the wall; it takes an infinite time for topographic Rossby waves carrying energy toward the wall to reach the apex of the escarpment. In the more general case, when the escarpment width is nonzero at the wall, an unsteady boundary layer will develop against the wall (Johnson and Davey, 1990). Energy carried toward the wall by long waves is in general, reflected as short waves. At large times, the flow is dominated by the waves of lowest frequency and the energy contained in the reflected waves is increasingly confined in the neighborhood of the wall. An analogous process occurs at the western boundary of the inviscid spin-up, in terms of linear Rossby waves, of a stratified fluid contained within a meridional channel on a local beta-plane (see Anderson and Gill, 1975). Dissipation allows a steady boundary layer to develop (Willmott and Johnson, 1979).

Johnson (1990) presents a method for explicitly obtaining the transmission amplitudes for Kelvin waves scattered by topography whose isobaths are parallel suffi-

ciently far from the vertical, but not necessarily planar, wall supporting the incident waves. The work generalizes the results in Johnson (1985), Gill *et al.* (1986) and Johnson and Davey (1990). Johnson (1990) considers the low-frequency limit and approximates continuous topography by a stepped feature, consisting of regions of constant height separated by vertical profiles. Killworth (1989) presents numerical simulations for the transmission of a coastal trapped Kelvin wave across a ridge which is perpendicular to the wall supporting the incident wave. However, numerical simulations are difficult to carry out, as noted by Killworth (1989), because over the downslope the field is dominated by short waves which are difficult to resolve on a numerical grid. The scattering of Kelvin waves by continuous, rather than stepped topography, is examined by Johnson (1993). In this paper Johnson is able to quantify the contribution of the short waves which occur, for example, where downslopes meet the bounding wall and presents a method of choosing the positions of the jumps when approximating complex topography. Johnson (1993) also presents an accurate estimate for the amplitude of the transmitted Kelvin waves in the problem addressed numerically by Killworth (1989).

Numerical studies of uniformly rotating flow across nonzero width escarpments have also been carried out by Wajsowicz (1991) and Allen (1988). Wajsowicz addresses the question of how deep water crosses the Greenland-Faeroes-Iceland ridge system using a primitive equation numerical model. Allen (1988) considers the adjustment of the free surface of a uniformly rotating homogeneous fluid in the presence of an infinitely long escarpment of nonzero width. After the passage of topographic Rossby waves, the fluid above the escarpment is found by Allen (1988) to be motionless, which is consistent with the conclusions of Willmott and Grimshaw (1991, 1992).

Johnson and Davey (1990) remove the restriction of the rigid-lid and consider the transient development to the steady flows described by Gill *et al.* (1986). For topography of small fractional height, two distinct time scales emerge. A fast time scale describing the adjustment to geostrophy of the initial unbalanced surface displacement and a slow, vortex-stretching time scale describing the subsequent evolution of the geostrophic state.

Apart from the studies of Allen (1988) and Wajsowicz (1991), all the above studies consider a homogeneous fluid. As a first step toward understanding the effects of stratification in the geostrophic adjustment problem with topography, this paper considers a 2-layer fluid with an infinitely long escarpment of small fractional depth, contained entirely within the lower layer. In this system two time scales emerge; a slow topographic (vortex stretching) time scale and the initial fast Poincaré and Kelvin wave time scale (Johnson and Davey, 1990). On the slow time scale, the fluid is brought to a steady geostrophic state after the passage of topographic Rossby wave, modified by stratification, along the step. Willmott and Johnson (1989) study the analogue of this wave in a uniformly rotating two-layer fluid contained within a circular basin with a step shelf.

Section 2 defines the problem and presents the solution, on the fast inertial time scale, of the initial unbalanced interfacial displacements to a state of geostrophy. During this rapid evolution the topography plays no role in the dynamics. However, on the slow vortex-stretching time scale the subsequent evolution to a steady state is achieved by the propagation of topographic Rossby waves, and this is described in Section 3. Final steady geostrophically adjusted solutions and solutions during the 'slow' adjustment phase are presented in Section 4. Finally, the results are discussed briefly in Section 5.

2. Statement of the problem and governing equations

Consider a uniformly rotating, inviscid, incompressible, two-layer fluid in which ρ_1 and ρ_2 are the uniform upper and lower layer densities respectively and H_1 is the depth of the undisturbed upper layer. With respect to a right-handed Cartesian coordinate frame $Ox^*y^*z^*$ an infinitely long step escarpment contained entirely within the lower layer lies along the x^*-axis (Fig. 1). The rigid lower boundary is given by $z^* = h_0 h(y)$ where h is order one. In this study $h = \text{sgn}y$ and $h_0 = \delta H^-/2$, where H^- is the total fluid depth in the region $y < 0$ and $\delta \ll 1$. In $y > 0$ the total fluid depth $H^+ = (1 - \delta)H^-$ and the average depth, H_0, of the fluid is given by $H_0 = (H^- + H^+)/2$.

Topographic compression of vortex filaments generates vorticity of order ϵf where $\epsilon = \delta H^-/(H_0 - H_1) \ll 1$ and $f/2$ is the constant angular speed of rotation of the fluid about a vertical axis (Johnson, 1984). The constraint on ϵ requires that the upper layer depth is thin, which is appropriate for oceanographic applications of this problem. Following Johnson and Davey (1990) the topographic vortex stretching time scale $T = (\epsilon f)^{-1}$ is therefore long compared to the inertial time f^{-1}.

The external Rossby radius of deformation associated with a fluid of depth H_0 is given by $r_e = (gH_0)^{1/2} f^{-1}$ where g is gravitational acceleration. Let η_0 be a surface displacement scale and $U = g\eta_0/(fr_e)$ be a velocity scale. With length scale r_e, and time scale f^{-1} and velocity scale U the nondimensional linear shallow water equations for a two-layer fluid become

$$\mathbf{u}_{1t} + \mathbf{k} \wedge \mathbf{u}_1 = -\nabla \eta_1, \tag{2.1}$$

$$(\eta_1 - \eta_2)_t + \left(\frac{H_1}{H_0}\right) \nabla \cdot \mathbf{u}_1 = 0, \tag{2.2}$$

$$\mathbf{u}_{2t} + \mathbf{k} \wedge \mathbf{u}_2 = -\nabla \eta_1 - \Delta \nabla \eta_2, \tag{2.3}$$

$$\eta_{2t} + \left(\frac{\overline{H}_2}{H_0}\right) \nabla \cdot \mathbf{u}_2 - \left(\frac{\overline{H}_2}{H_0}\right) \epsilon \nabla \cdot (h\mathbf{u}_2) = 0, \tag{2.4}$$

where

$$\Delta = (\rho_2 - \rho_1)/\rho_2,$$

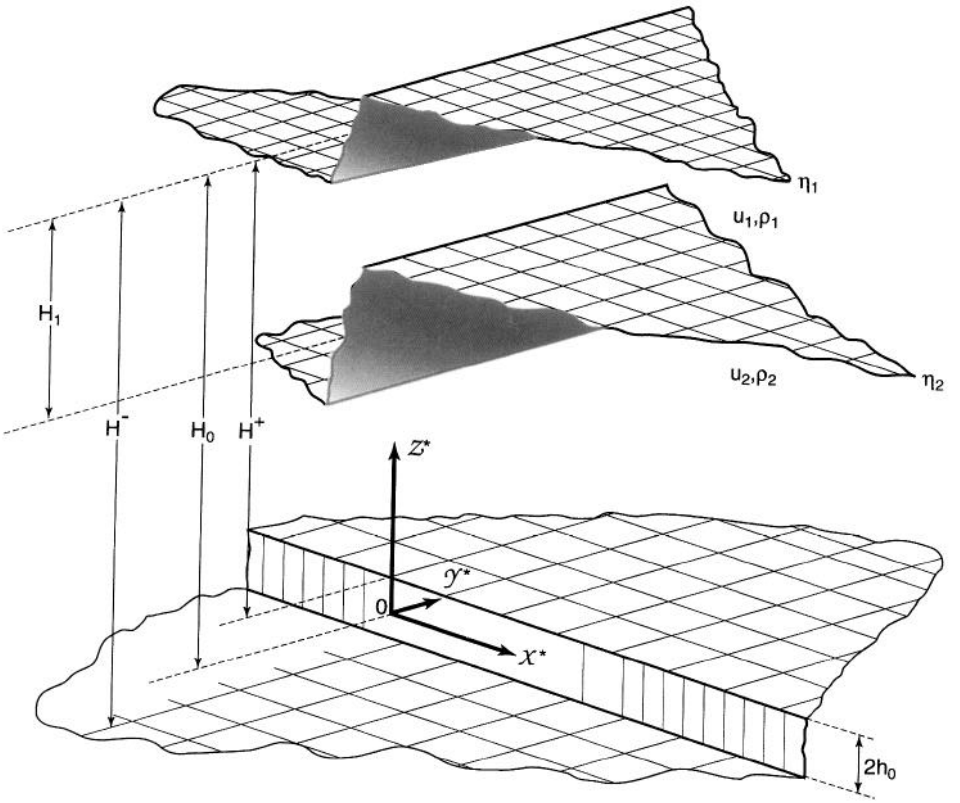

Figure 1. The geometry of the uniformly rotating two layer-fluid above an infinitely long step escarpment of height $2h_0$ located at $y^* = 0$. Initially the fluid is at rest with average fluid depth in $y^* > 0$ equal to H^+ and in $y^* < 0$, H^-. The undisturbed upper layer depth is H_1. Initially at least one interface has a step discontinuity along $x^* = 0$ (i.e. perpendicular to the escarpment). In the example shown in the sketch, the initial free surface $\eta_1 = \eta_0 \operatorname{sgn}(x)$ and the initial interfacial displacement $\eta_2 = \eta_0 \Delta^{-1} \operatorname{sgn}(x)$.

is the stratification parameter, $\mathbf{u}_i = (u_i, v_i)$ is the horizontal velocity in the i^{th} layer (with $i = 1$ denoting the upper layer), $\overline{H}_2 = H_0 - H_1$ is the average depth of the lower layer and $\mathbf{k}$ is a unit vector along the Oz direction. Since the upper layer depth is 'thin' $(\overline{H}_2/H_0)$ is an order one quantity. The upper and lower layer vorticity equations, formed from (2.1) and (2.3) respectively, are given by

$$\left[v_{1x} - u_{1y} + \frac{H_0}{H_1}(\eta_2 - \eta_1)\right]_t = 0, \tag{2.5a}$$

$$(v_{2x} - u_{2y})_t + \epsilon \nabla \cdot (h\mathbf{u}_2) - \left(\frac{H_0}{\overline{H}_2}\right)\eta_{2t} = 0. \tag{2.5b}$$

Initially the fluid is at rest and at least one interface has a step discontinuity along

$x = 0$ (i.e. perpendicular to the step topography). Therefore

$$\left.\begin{aligned} &u_i = 0 = v_i, \\ &\eta_1 = \gamma_1 \operatorname{sgn}(x), \qquad \Delta\eta_2 = \gamma_2 \operatorname{sgn}(x), \end{aligned}\right\} \text{at } t = 0, \tag{2.6}$$

where γ_i take the values 0, ± 1. When $\gamma_i = 0$, the i^{th} interface is initially flat. The classical Rossby adjustment problem takes place on the fast time scale t. Internal-inertial waves and external Poincaré waves play a role on the fast adjustment to geostrophy followed by a slow evolution on the time-scale T controlled by topographic Rossby waves.

a. The rapid inertial adjustment. The vorticity equations (2.5) in the limit $\epsilon \to 0$ with t fixed are integrated with respect to time to yield

$$v_{1x} - u_{1y} + \left(\frac{H_0}{H_1}\right)(\eta_2 - \eta_1) = \left(\frac{H_0}{H_1}\right)(\gamma_2\Delta^{-1} - \gamma_1) \operatorname{sgn}(x), \tag{2.7a}$$

$$v_{2x} - u_{2y} - \left(\frac{H_0}{H_2}\right)\eta_2 = -\left(\frac{H_0}{H_2}\right)\gamma_2\Delta^{-1} \operatorname{sgn}(x), \tag{2.7b}$$

after application of (2.6). As noted by Johnson and Davey (1990) the effects of topography vanish in this limit. Steady geostrophic y-independent solutions of (2.7) exist in which

$$v_1 = \eta_{1x}, \qquad v_2 = (\eta_1 + \Delta\eta_2)_x, \tag{2.8a}$$

with

$$\eta_{1xx} + \left(\frac{H_0}{H_1}\right)(\eta_2 - \eta_1) = \left(\frac{H_0}{H_1}\right)(\gamma_2\Delta^{-1} - \gamma_1) \operatorname{sgn}(x), \tag{2.8b}$$

$$\begin{aligned} \Delta\eta_{2xx} - \left(\frac{H_0}{H_2}\right)\eta_2 - \left(\frac{H_0}{H_1}\right)(\eta_2 - \eta_1) = &-\frac{H_0}{H_2}\gamma_2\Delta^{-1} \operatorname{sgn}(x) \\ &- \frac{H_0}{H_1}(\gamma_2\Delta^{-1} - \gamma_1) \operatorname{sgn}(x). \end{aligned} \tag{2.8c}$$

The solution of (2.8b,c) is readily obtained using modal variables $\eta^{(n)} (n = 1, 2)$ where

$$\eta^{(n)} = \eta_1 + q^{(n)}\eta_2, \tag{2.9a}$$

and $q^{(n)}$ are modal coefficients which satisfy

$$q^2 + q\left[\frac{H_0}{H_2} - \Delta\right] - \Delta = 0, \tag{2.9b}$$

with the positive root defined as $q^{(1)}$. In terms of $\eta^{(n)}$ (2.8b,c) can be expressed in the

decoupled form

$$\eta_{xx}^{(n)} - \left[\frac{1}{r^{(n)}}\right]^2 \eta^{(n)} = -\frac{(\gamma_1 + q^{(n)}\gamma_2\Delta^{-1})}{[r^{(n)}]^2}\,\mathrm{sgn}\,(x), \tag{2.10a}$$

where the separation constant $r^{(n)}$ is given by

$$\left[\frac{1}{r^{(n)}}\right]^2 = \frac{H_0}{H_1}\left(1 - \frac{q^{(n)}}{\Delta}\right). \tag{2.10b}$$

It follows from (2.10) that the steady bounded geostrophically adjusted flow, in the limit $t \to \infty$, is given by

$$\eta_1 = \gamma_1\,\mathrm{sgn}\,(x) + \frac{1}{\Delta q}\left[q^{(2)}A_1 e^{-|x|/r^{(1)}} - q^{(1)}A_2 e^{-|x|/r^{(2)}}\right]\mathrm{sgn}\,(x), \tag{2.11a}$$

$$\eta_2 = \gamma_2\Delta^{-1}\,\mathrm{sgn}\,(x) + \frac{1}{\Delta q}\left[A_2 e^{-|x|/r^{(2)}} - A_1 e^{-|x|/r^{(1)}}\right]\mathrm{sgn}\,(x), \tag{2.11b}$$

where

$$A_1 = -\gamma_1 - \gamma_2\Delta^{-1}q^{(1)}, \qquad A_2 = -\gamma_1 - \gamma_2\Delta^{-1}q^{(2)},$$

and

$$\Delta q = q^{(2)} - q^{(1)}.$$

The solution (2.11) describes geostrophic jets in each layer which are symmetric about $x = 0$ (the location of the initial interfacial discontinuities) and hence perpendicular to the step. Steady geostrophic flow cannot cross isobaths. On the longer vortex-stretching time scale (2.11) will adjust via the propagation of topographic Rossby waves, to a steady state which is compatible with the topography.

3. Slow, topographic adjustment

Consider (2.1) to (2.4) in the limit $\epsilon \to 0$ on the topographic vortex stretching time scale $\tau = \epsilon t$ fixed. Then (2.1) and (2.3) reduce to the geostrophic balance equations

$$\mathbf{k} \wedge \mathbf{u}_1 = -\nabla\eta_1, \tag{3.1a}$$

$$\mathbf{k} \wedge \mathbf{u}_2 = -\nabla\eta_1 - \Delta\nabla\eta_2, \tag{3.1b}$$

while (2.5a) and (2.5b) become

$$\nabla^2\eta_{1\tau} + \left(\frac{H_0}{H_1}\right)(\eta_2 - \eta_1)_\tau = 0 \tag{3.2a}$$

$$\nabla^2(\eta_1 + \Delta\eta_2)_\tau - \frac{H_0}{H_2}\eta_{2\tau} + J(\eta_1 + \Delta\eta_2, h) = 0, \tag{3.2b}$$

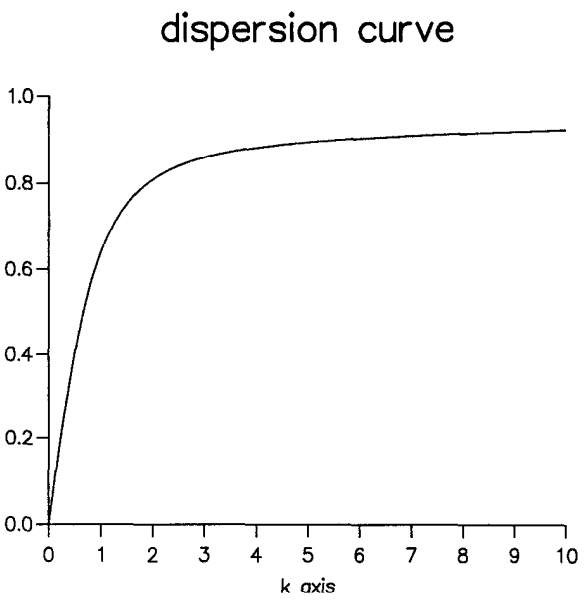

Figure 2. Plot of the dispersion relation (3.13b) for topographic Rossby waves, modified by stratification, which are trapped over the step escarpment. The waves are more frequently called internal double Kelvin waves. Parameter values used are given in Appendix B.

where J denotes the Jacobian operator. The adjusted solutions (2.11) are the initial conditions for (3.2). Let $\eta_{10}(x)$ and $\eta_{20}(x)$ denote the adjusted solutions for η_1 and η_2 respectively given by (2.11), and $\psi_j = \eta_j - \eta_{j0}$ denote the deviation from the initial geostrophically adjusted elevations, where $j = 1, 2$. In terms of ψ_j the topographic adjustment problem becomes

$$\nabla^2\psi_{1t} + \left(\frac{H_0}{H_1}\right)(\psi_2 - \psi_1)_t = 0, \tag{3.3a}$$

$$\nabla^2(\psi_1 + \Delta\psi_2)_t - \frac{H_0}{H_2}\psi_{2t} + J(\psi_1 + \Delta\psi_2, h) = -J(\eta_{10} + \Delta\eta_{20}, h), \tag{3.3b}$$

with

$$\psi_1 = 0 = \psi_2 \qquad \text{at} \qquad t = 0. \tag{3.4}$$

In (3.3) and (3.4) and the remainder of this section the topographic time scale τ has been replaced by t for notational convenience. Matching conditions across the step are

$$[\psi_1] = 0 = [\psi_2] \qquad \text{on} \qquad y = 0, \tag{3.5}$$

$$[\psi_{1y t}] = 0 \qquad \text{on} \qquad y = 0, \tag{3.6}$$

$$\Delta[\psi_{2y t}] + (\psi_1 + \Delta\psi_2)_x[h] = -V_0[h], \tag{3.7}$$

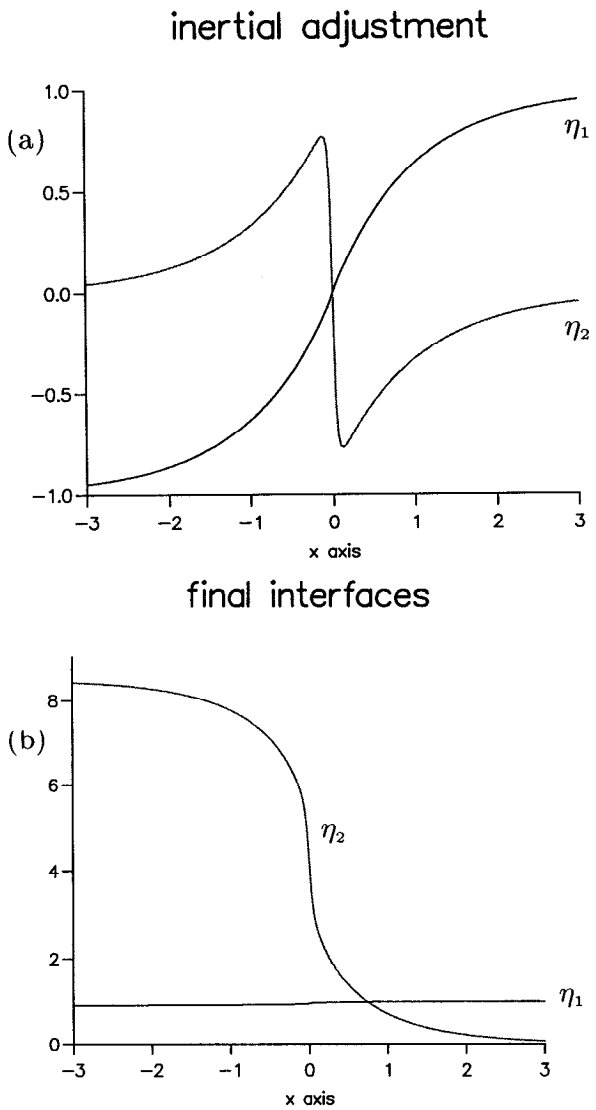

Figure 3. (a) Free surface (η_1) and interfacial (η_2) displacements over the step (i.e. along $y = 0$) following the rapid inertial adjustment from the initial state $\eta_1 = \text{sgn}(x)$, $\eta_2 = 0$; (b) Final steady free surface and interfacial displacements over the step which are established after the passage of internal double Kelvin waves.

where

$$V_0(x) \equiv (\eta_{10} + \Delta\eta_{20})_x,$$

is the initial cross-step flow and $[\cdot]$ denotes the jump in the enclosed quantity across the step. Matching conditions (3.5) express continuity of pressure across the step.

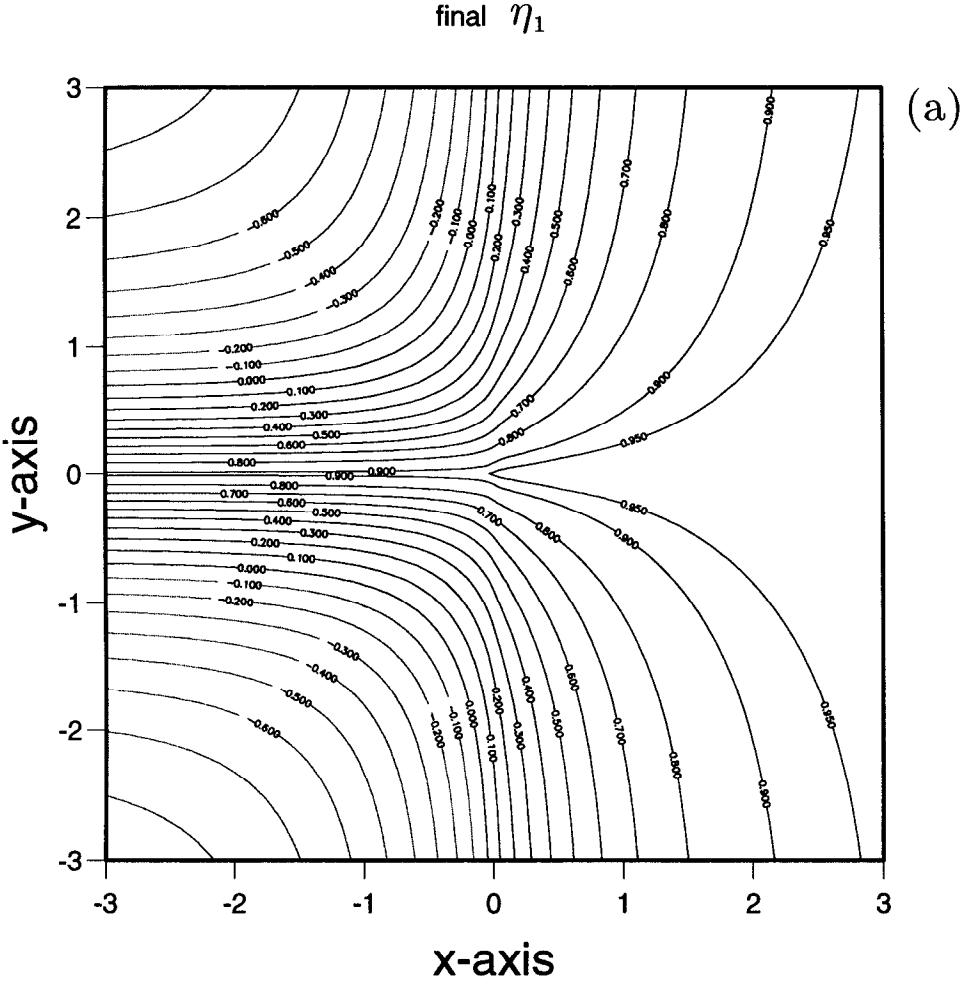

Figure 4. Contour plots of (a) final steady free surface displacement, η_1, which is the upper layer streamfunction; (b) final steady interfacial displacement η_2; (c) the lower layer streamfunction $\eta_1 + \Delta\eta_2$ in the steady state. In (a) and (c) the evenly spaced contour increment is 0.1, with the exception of contour level 0.95.

Matching conditions (3.6) and (3.7) are obtained by integrating (3.2a) and (3.2b) with respect to y over the interval $[-\epsilon, \epsilon]$ followed by taking the limit as $\epsilon \to 0$, respectively. In physical terms (3.6) and (3.7) express continuity of cross-step transport in each layer. From (3.6) it is also clear that only one family of subinertial waves contributes to the topographic adjustment, namely topographic Rossby waves modified by stratification (Rhines, 1977; Willmott, 1984; Willmott and Johnson, 1989).

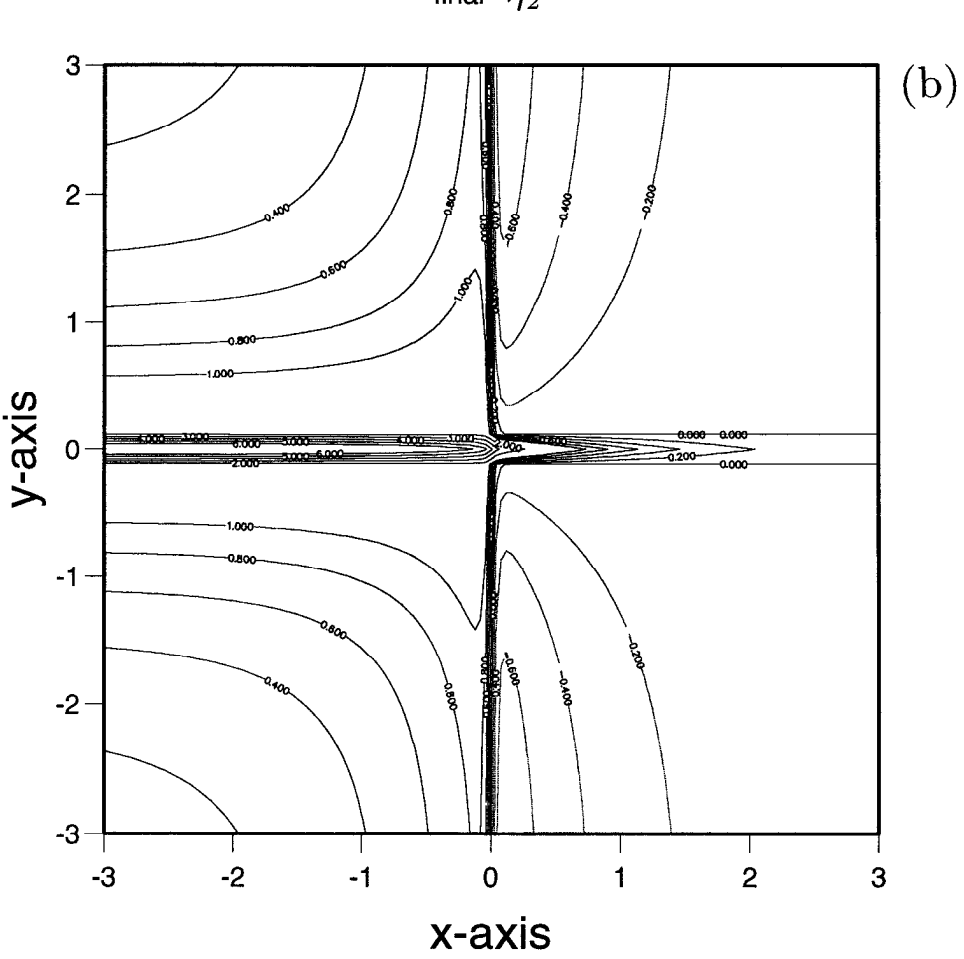

Figure 4. (Continued)

Integrating (3.3) and (3.6) with respect to time and employing (3.5) yields

$$\nabla^2\psi_1 + \frac{H_0}{H_1}(\psi_2 - \psi_1) = 0, \tag{3.8a}$$

$$\nabla^2(\psi_1 + \Delta\psi_2) - \frac{H_0}{H_2}\psi_2 = 0, \tag{3.8b}$$

with

$$[\psi_{1y}] = 0, \qquad \text{on } y = 0, \tag{3.9}$$

$$\Delta[\psi_{2yt}] + 2s(\psi_1 + \Delta\psi_2)_x = -2sV_0, \qquad \text{on } y = 0, \tag{3.10}$$

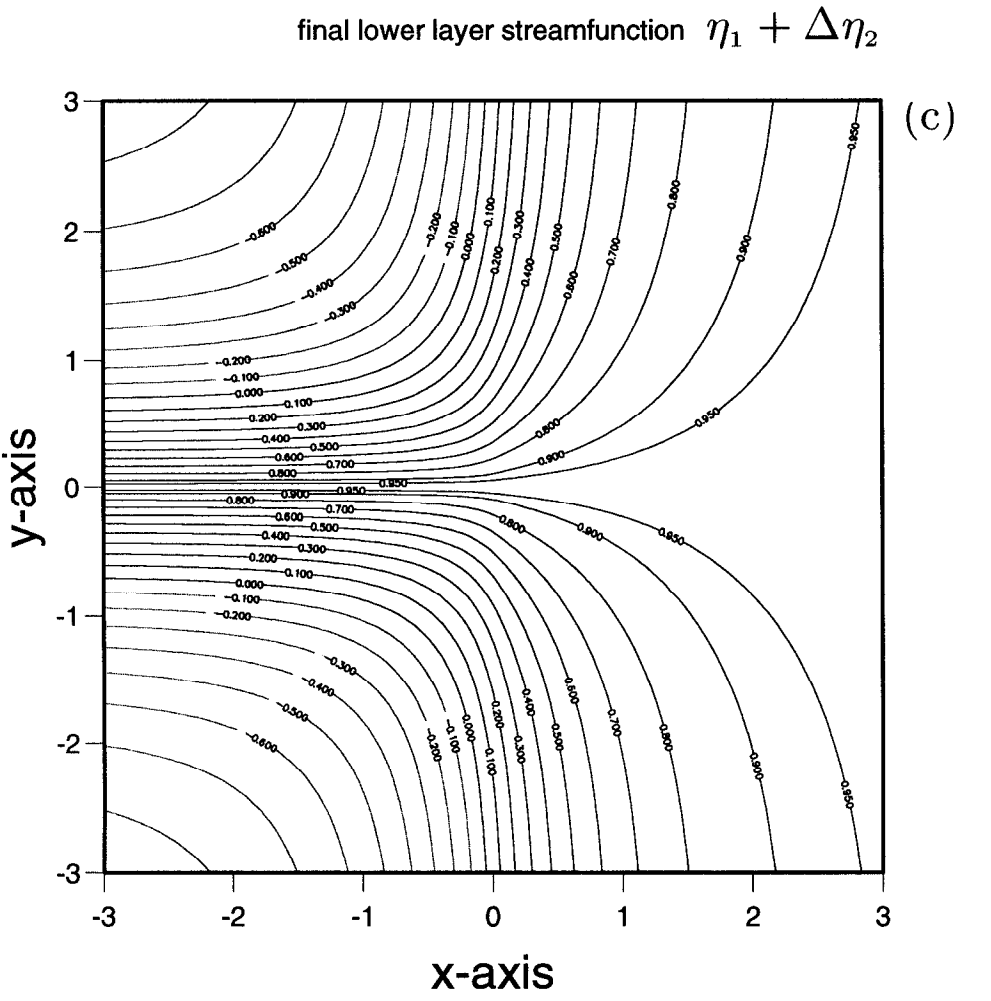

Figure 4. (Continued)

for the step escarpment $h(y) = s \text{ sgn } (y)$, where $s = \pm 1$. The solution of (3.8) subject to (3.5), (3.9) and (3.10) is readily obtained using the modal variable approach in Section 2. In terms of the modal variables $\psi^{(n)} = \psi_1 + q^{(n)}\psi_2$ $(n = 1, 2)$,

$$\psi_1 = (\Delta q)^{-1}[q^{(2)}\psi^{(1)} - q^{(1)}\psi^{(2)}], \qquad \psi_2 = (\Delta q)^{-1}[\psi^{(2)} - \psi^{(1)}], \tag{3.11}$$

where $q^{(n)}$ are the roots of the quadratic (2.9b). Let subscripts N and P denote variables in $y < 0$ and $y > 0$ respectively. Then the solution for the modal variables which satisfy the matching conditions (3.5), (3.9) and (3.10) and the initial conditions

(3.4) is given by

$$\psi_N^{(1)} = \frac{1}{2\pi}\int_{-\infty}^{\infty} \frac{q^{(1)}}{K_1} A(k,t) \exp\,[ikx + K_1 y]dk, \tag{3.12a}$$

$$\psi_N^{(2)} = \frac{1}{2\pi}\int_{-\infty}^{\infty} \frac{q^{(2)}}{K_2} A(k,t) \exp\,[ikx + K_2 y]dk, \tag{3.12b}$$

$$\psi_P^{(1)} = \frac{1}{2\pi}\int_{-\infty}^{\infty} \frac{q^{(1)}}{K_1} A(k,t) \exp\,[ikx - K_1 y]dk, \tag{3.12c}$$

$$\psi_P^{(2)} = \frac{1}{2\pi}\int_{-\infty}^{\infty} \frac{q^{(2)}}{K_2} A(k,t) \exp\,[ikx - K_2 y]dk, \tag{3.12d}$$

where

$$A_t - i\Omega(k)A = \frac{s}{\Delta}\overline{V}_0, \qquad A = 0 \text{ at } t = 0, \tag{3.13a}$$

$$\Omega(k) = \frac{sk\hat{K}}{(\Delta q)K_1K_2}, \tag{3.13b}$$

with

$$\hat{K} \equiv K_1(1 + q^{(2)}) - K_2(1 + q^{(1)}),$$

and

$$K_1^2 = k^2 + [r^{(1)}]^{-2}, \qquad K_2^2 = k^2 + [r^{(2)}]^{-2}.$$

In (3.13a), $\overline{V}_0$ denotes the complex Fourier transforms of V_0. Clearly $\Omega(k)$ is the frequency of the topographic Rossby waves; a plot of the wave dispersion relation (3.13b) is shown in Figure 2 using parameter values listed in Appendix B. At long wavelengths (i.e. $k \to 0$) the waves are nondispersive, while (3.13b) shows that $\Omega(k) \to s$ as $k \to \infty$. It is clear from Figure 2 that the waves propagate energy unidirectionally at all wavelengths.

The solution of (3.13a) is given by

$$A(k,t) = A_{PI}(1 - e^{i\Omega t}), \tag{3.14}$$

where

$$A_{PI}(k) = \frac{i(\Delta q)K_1K_2\overline{V}_0}{k\Delta\hat{K}}.$$

In terms of the Fourier transform $\overline{\eta}_0 \equiv \overline{(\eta_{10} + \Delta\eta_{20})}$, A_{PI} can be rewritten as

$$A_{PI}(k) = -\frac{(\Delta q)K_1K_2}{\Delta\hat{K}}\overline{\eta}_0.$$

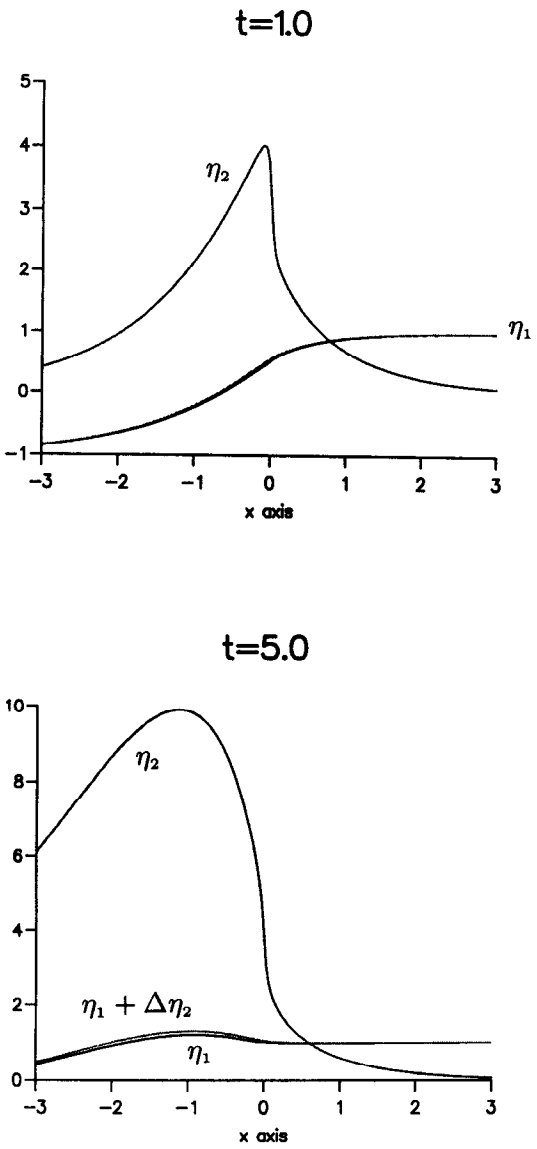

Figure 5. Plot of the free surface and interfacial displacements and $\eta_1 + \Delta\eta_2$ above the step at $t = 1$, 5, 10 and 20, showing how the internal double Kelvin wave establishes the steady solutions in Figure 3(b). The plot of $\eta_1 + \Delta\eta_2$ almost coincides with η_1 at $t = 1$, 20 and is therefore not labelled.

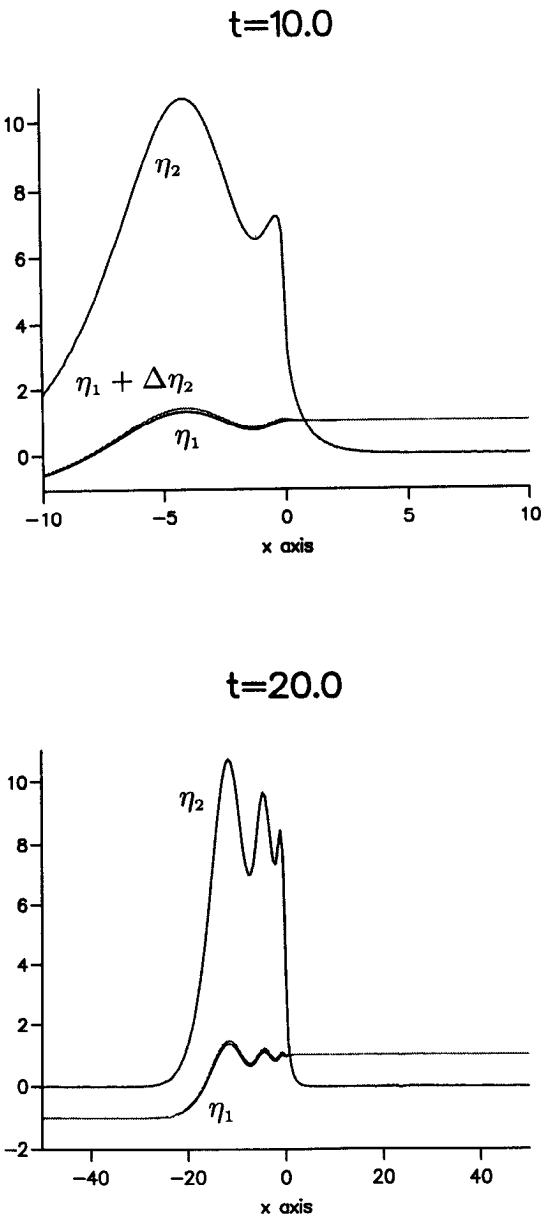

Figure 5. (Continued)

Using (3.14), the modal fields (3.12a to d) are therefore determined, and the interfacial displacements can be calculated from (3.11). From (2.11) it can be shown that

$$\overline{V}_0 = \frac{2H_0}{\Delta\overline{H}_2K_1^2K_2^2}\left[\gamma_2k^2 + \frac{H_0}{H_1}(\gamma_1 + \gamma_2)\right]. \tag{3.15}$$

Evaluation of the Fourier integrals (3.12a to d) requires care and Appendix A describes the method adopted. In particular, over the escarpment ($y = 0$) the steady contribution from (3.12a) which emerges as $t \to \infty$ is given by

$$\lim_{t\to\infty} \psi^{(1)}(x, 0, t) \equiv \psi_s^{(1)}(x) = \frac{1}{\pi}\int_0^1 \left[\frac{\hat{A}_{PI}(k) - \hat{A}_{PI}(0)}{k}\right] \sin(kx)dk + \frac{1}{\pi}\int_1^\infty \frac{\hat{A}_{PI}(k)}{k} \sin(kx)dk + \frac{1}{\pi}\hat{A}_{PI}(0)Si(x) - \frac{1}{2}\hat{A}_{PI}(0), \tag{3.16}$$

where $A_{PI}(k) \equiv \hat{A}_{PI}/k$ and Si denotes the sine integral. The form (3.16) is suitable for numerical evaluation. All integrals in (3.16) are proper and in the second integral on the right-hand side of this expression, $\hat{A}_{PI}(k)/k \sim k^{-5}(\gamma_2 = 0)$ or $k^{-3}(\gamma_2 \neq 0)$ as $k \to \infty$, which enables accurate numerical evaluation. The steady contributions from (3.12b to d) as $t \to \infty$ are evaluated in a similar way.

4. Results

Figure 3(a) shows plots of the interfacial displacements given by (2.11) which are established at the end of the "rapid" inertial adjustment phase when $\gamma_1 = 1.0$ and $\gamma_2 = 0$. Initially there is a step in the surface interface, while the lower interface is flat. After the rapid adjustment phase, both interfaces are odd functions of x (see (2.11)), with η_1 adjusting to the initial "far field" value $+1$ as $x \to \infty$ on the external Rossby radius scale r_e. However, η_2 varies over the short length scale, $r_i = (g'H_1\overline{H}_2/H_0)^{1/2}f^{-1}$, in the neighborhood of the origin, and decays exponentially to zero as $|x| \to \infty$ on the e-folding length scale r_e.

After the passage of the topographic Rossby waves, a plot of the final steady interfaces above the escarpment is shown in Figure 3(b). In the steady state, (3.1) shows that η_1 and $\eta_1 + \Delta\eta_2$ are the upper and lower layer geostrophic streamfunctions, respectively. Over the step $\eta_1 + \Delta\eta_2$ is constant, which is seen in contours of this field in Figure 4(c), and there is no cross-step transport in the lower layer. In this sense the lower layer adjusts in a similar manner to a single homogeneous layer above topography, as discussed by Johnson (1985), Gill *et al.* (1986) and Willmott and Grimshaw (1991, 1992). Weak cross-step flow is established in the upper layer (see Fig. 4(a)). In the steady state the amount of fluid in the upper layer that crosses the step, rather than being deflected (to the left) along the step to cross at $x = -\infty$ is

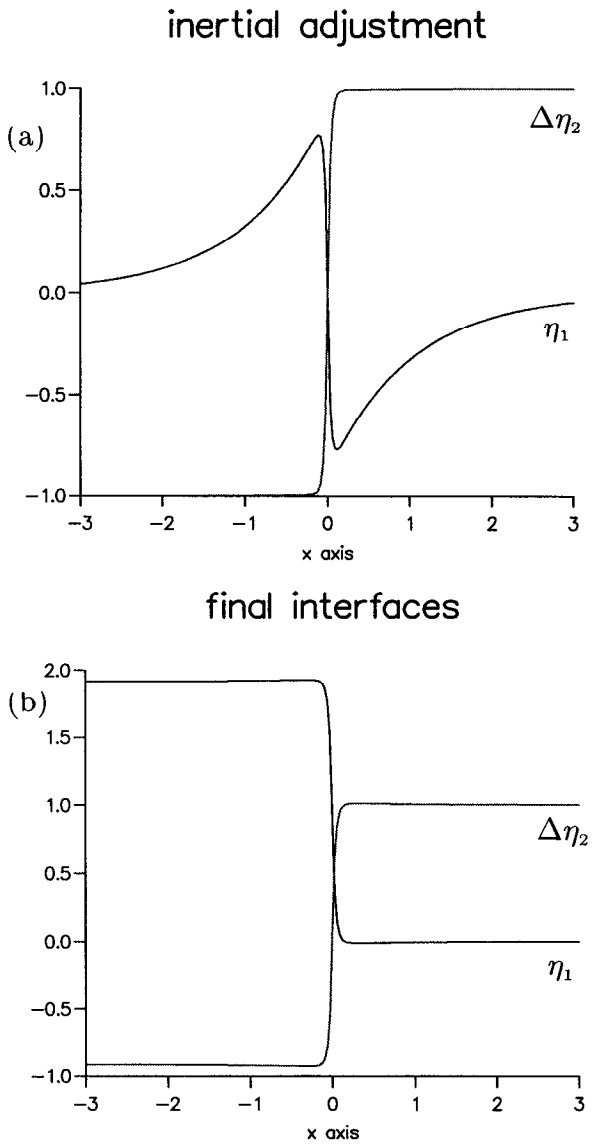

Figure 6. As in Figure 3, except $\Delta\eta_2$ rather than η_2 is plotted and the initial conditions are $\eta_1 = 0, \Delta\eta_2 = \text{sgn}\,(x)$.

simply, $\lim_{x\to-\infty}(\Delta\eta_2) \approx 0.075$. Figure 4(a) confirms that most of the fluid does not cross the step within a finite distance.

Since topographic Rossby waves propagate information unidirectionally (in the negative x-direction for this topography), as $x \to \infty$ the interfaces η_1 and η_2 tend to the values γ_1 and $\gamma_2\Delta^{-1}$ respectively. Above the step (i.e. on $y = 0$) the final steady

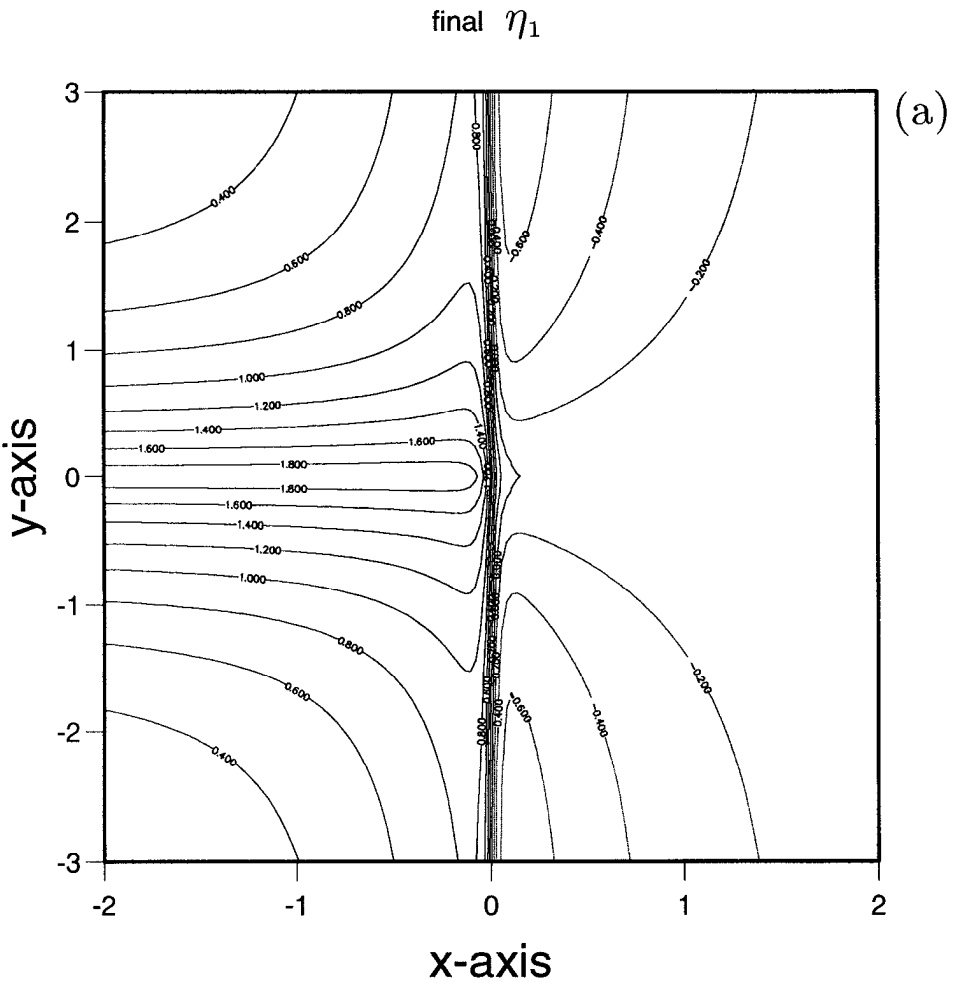

Figure 7. Contour plots (a) to (c) as in Figure 4, except that the initial conditions of Figure 6 are used. Surface plots of η_1, $\Delta\eta_2$ and $\eta_1 + \Delta\eta_2$ in the final steady state are shown in (d), (e) and (f) respectively. In (a) and (c) the evenly spaced contour increment is 0.2. Contour levels ± 0.95, ± 0.9, ± 0.6, ± 0.3 and 0 are plotted in (b).

solution for η_2 adjusts from the "upstream" value of $\gamma_2\Delta^{-1}$ (which is zero in this example) to a uniform "downstream" value, over the length scale r_e (see Figs. 3(b) and 4(b)). This adjustment length scale is a feature common to all the final steady solutions for η_2, irrespective of the values of γ_1 and γ_2.

Evolution of the interfacial displacements above the step at various values of the topographic adjustment time scale are shown in Figure 5. Also plotted in Figure 5 is $\eta_1 + \Delta\eta_2$, although for this example this curve almost overlaps with the plot of η_1 because the latter is almost uniform above the step (see Figure 3(b)). On each curve

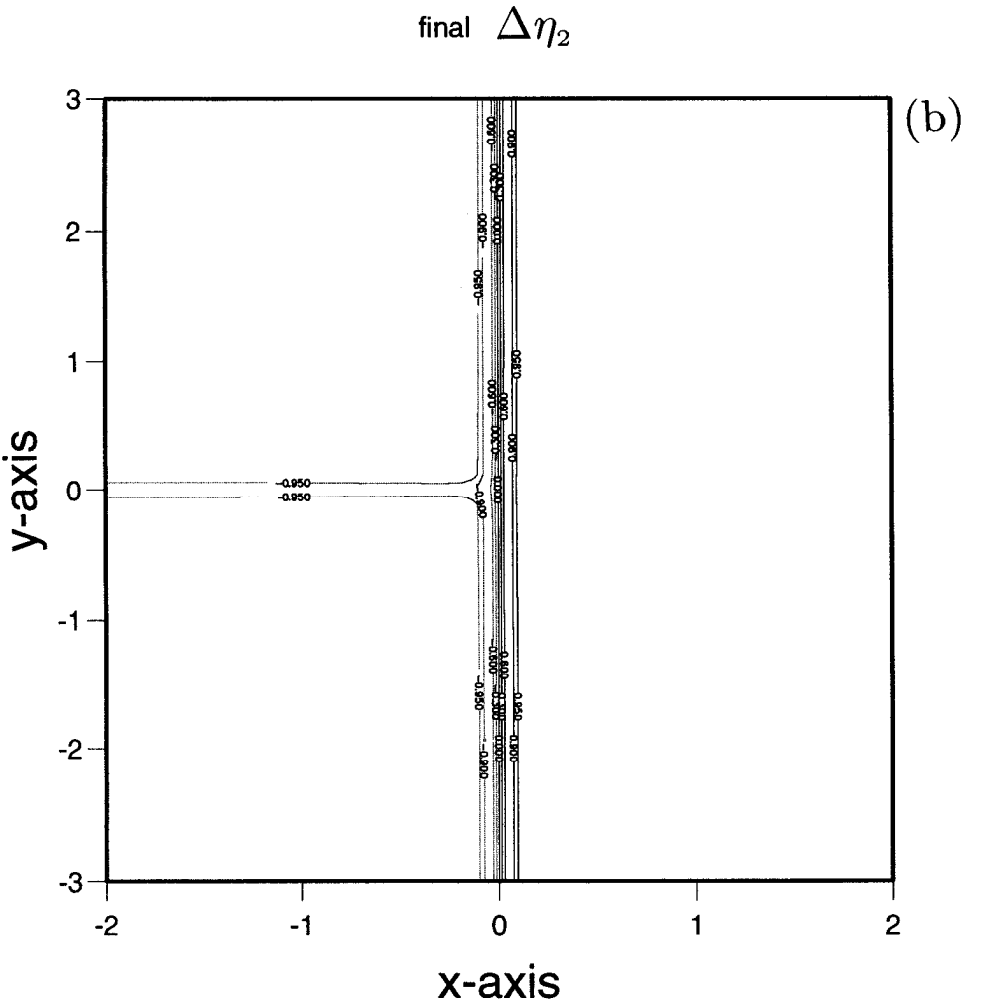

Figure 7. (Continued)

a leading wavefront propagates at speed $c_g(0) = d\Omega(0)/dk$; behind each wavefront a tail of dispersive waves is formed which oscillate about the final steady values.

A plot of the interfacial displacements above the step, after the "rapid" inertial adjustment has taken place, is shown in Figure 6(a) for the case $\gamma_1 = 0$ and $\gamma_2 = 1.0$. Figure 6(a) shows that the upper layer flow consists of an intense symmetric jet centered about $x = 0$, flowing in the negative y-direction. The characteristic width of this jet is given by r_i. On either side of the narrow jet are broad (characteristic width r_e) currents flowing in the positive y-direction. The final steady geostrophically adjusted interfaces above the step (see Figure 6(b)) together with contour and surface plots of the steady interfaces (see Figure 7) show that after the passage of the

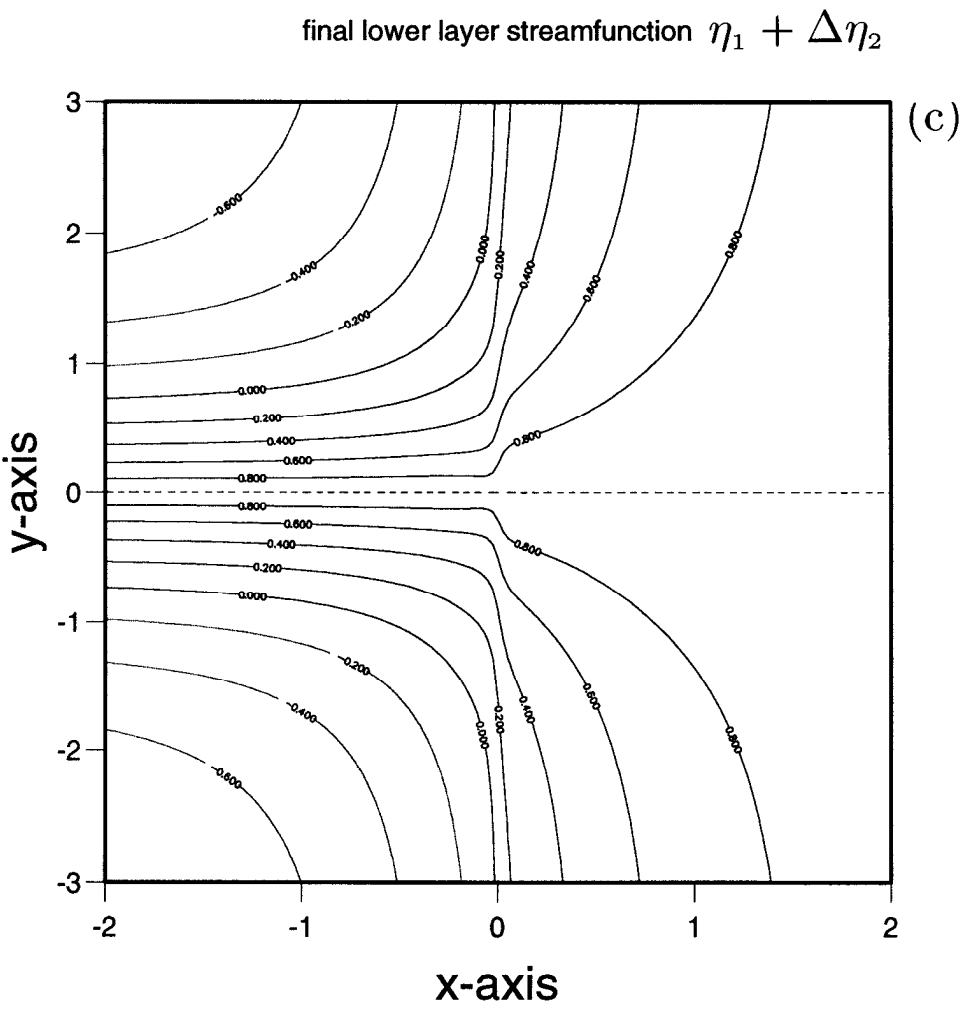

Figure 7. (Continued)

internal double Kelvin wave the topography blocks the upstream cross-step flow in the positive y-direction within the upper layer. Cross-step flow in the upper layer continues in the negative y-direction within the narrow jet centered around $x = 0$. In $x < 0$, flow in the narrow jet is augmented on either side of the step by fluid within semi-closed circulation cells that are formed when the topography blocks the upstream broad cross-step current. It can also be deduced from Figure 7(a) that in $x < 0$ a closed upper layer anticyclonic circulation occurs over the step at finite time. As the wavefront of the internal double Kelvin wave propagates toward $x = -\infty$, the width of the anticyclonic circulation increases because within the gyre, cross-step flow in the positive y-direction occurs in the neighborhood of the advancing wave-

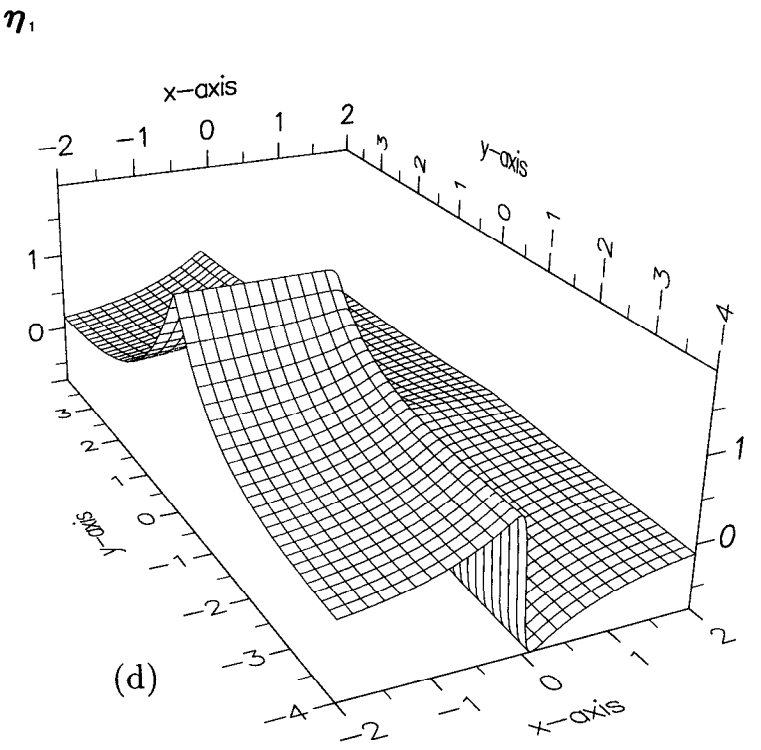

Figure 7. (Continued)

front. Therefore in the final steady state (see Fig. 7a) the upper layer anticyclonic circulation is blocked by the topography.

The final steady solution for η_2 is controlled by the passage of the internal double Kelvin wave. Figures 6(b) and 7(b) show that over the step η_2 and η_{2x} vary on the scale r_i. Since $\eta_1 + \Delta\eta_2$ is constant over the step in the final steady state (the constant is unity in this example) η_1 and η_{1x} also vary on the scale r_i leading to the intense cross-step current (see Fig. 7a). Figure 7(c) confirms that cross-step flow in the lower layer is blocked by the step.

In the case when both interfaces initially have step discontinuities perpendicular to the escarpment (i.e. $\gamma_1 = \gamma_2 = 1$), Figures 8(a) and (b) show the interfaces after the rapid inertial adjustment and the final steady solutions above the step, respectively. Also shown in Figure 8(b) is a plot of the curve $\eta_1 + \Delta\eta_2$ above the step, which has the constant value 2, corresponding to the initial value of this field far "upstream." Figure 9 shows contour plots of η_1 and $\eta_1 + \Delta\eta_2$ in the final steady state and these can be constructed from the addition of the solutions in the two previous examples (i.e. superposition of the contour fields in Figures 4 and 7). Again the robust features of the solution are blocked cross-step lower layer transport and a "narrow" cross-step geostrophic jet in the upper layer.

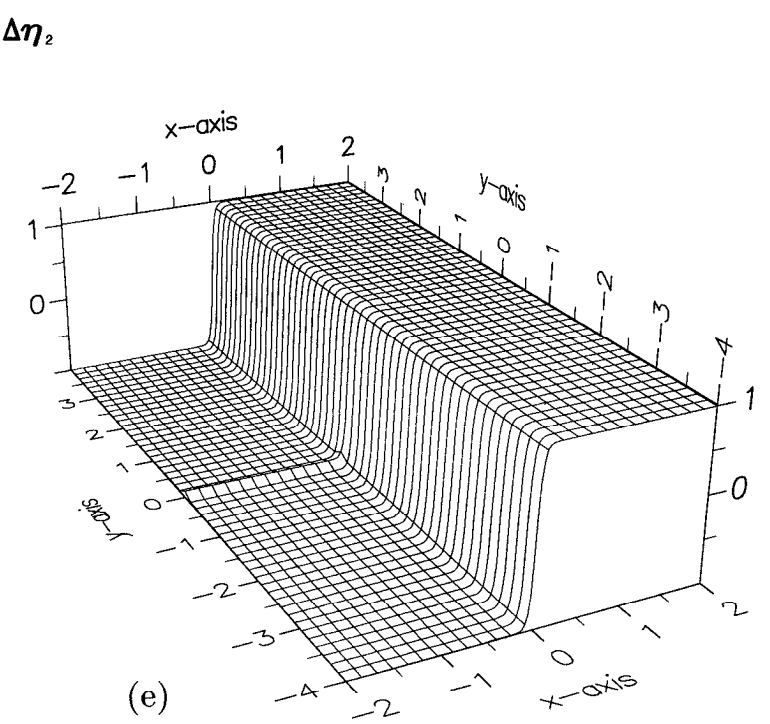

Figure 7. (Continued)

5. Summary and discussion

This paper examines the linear Rossby adjustment problem for an inviscid two-layer fluid in the presence of an infinitely long step escarpment, the height of which is assumed to be infinitesimal compared to the average depth of the lower layer. For this case the vortex stretching time scale is long compared to the inertial time scale and this facilitates an analytical treatment of the problem.

Initially the free surface and interfacial displacements have step discontinuities perpendicular to the step and the fluid is at rest with respect to the coordinate frame. If the flow is governed by the linear shallow water equations, how does the fluid evolve upon releasing the interfaces? The analogous problem has been considered by Gill *et al.* (1986) for a homogeneous fluid with a step escarpment. Gill *et al.* (1986) found that the fluid evolves to a steady geostrophic state in which no fluid can cross the step. A steady geostrophic state is expected to emerge for the two-layer problem, in which case it can be anticipated that the lower layer will behave in a manner qualitatively similar to the solution obtained by Gill *et al.* (1986). However, does the topography block the upper layer geostrophic flow in the steady limit?

Following Johnson and Davey (1990), a two time-scale method shows that the rapid inertial adjustment of the fluid, via propagation of external and internal Poincaré waves, is unaffected by the topography. On the slow vortex stretching time

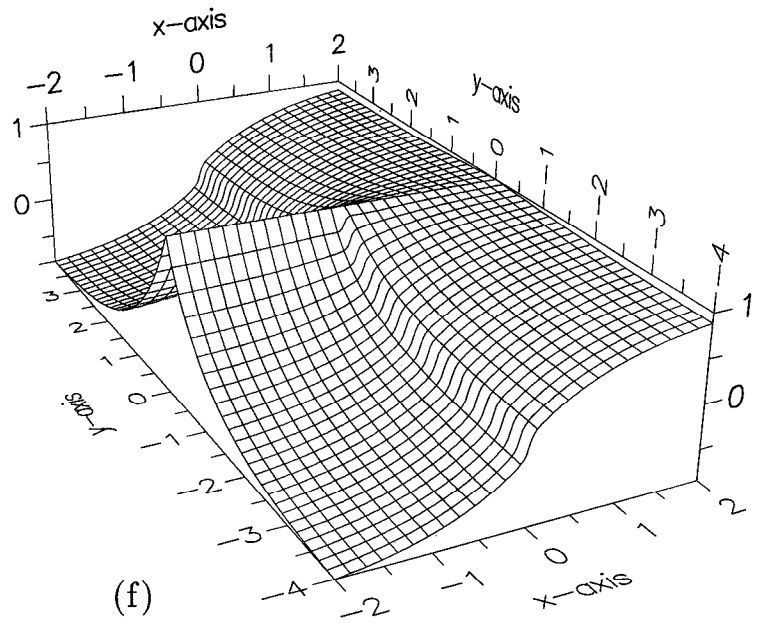

Figure 7. (Continued)

scale a steady solution is established after the passage of the topographic Rossby waves (which are commonly referred to as internal double Kelvin waves when the trapping topography is an escarpment). A jet, of characteristic width r_i (the internal Rossby radius) crosses the step in the upper layer in the final steady state. However, the majority of the upper layer fluid is blocked by the step; the amount of fluid which crosses the step is given by the value of $\Delta\eta_2$ far "downstream," where Δ is the stratification parameter and η_2 is the interfacial displacement. "Downstream" refers to the direction in which the Rossby waves propagate, which in this paper is the negative x-direction. The results of this study support the idea that stratification tends to shelter the upper oceanic flow from the influence of topography.

Gill *et al.* (1986) describe results from a rotating tank experiment in which a coastal jet in a two-layer fluid is forced to cross an escarpment which intersects a vertical coastal wall at right angles. Initially the free surface is flat and the interfacial displacement has a step (maintained by a vertical barrier) parallel to the coastal wall. Upon removal of the barrier a buoyancy driven coastal jet is established which is deflected offshore or onshore over the step escarpment depending on the geometry of the topography. Gill *et al.* (1986) note that the flow set up in the lower layer is in the opposite direction to that in the upper layer. The same vertical structure in the

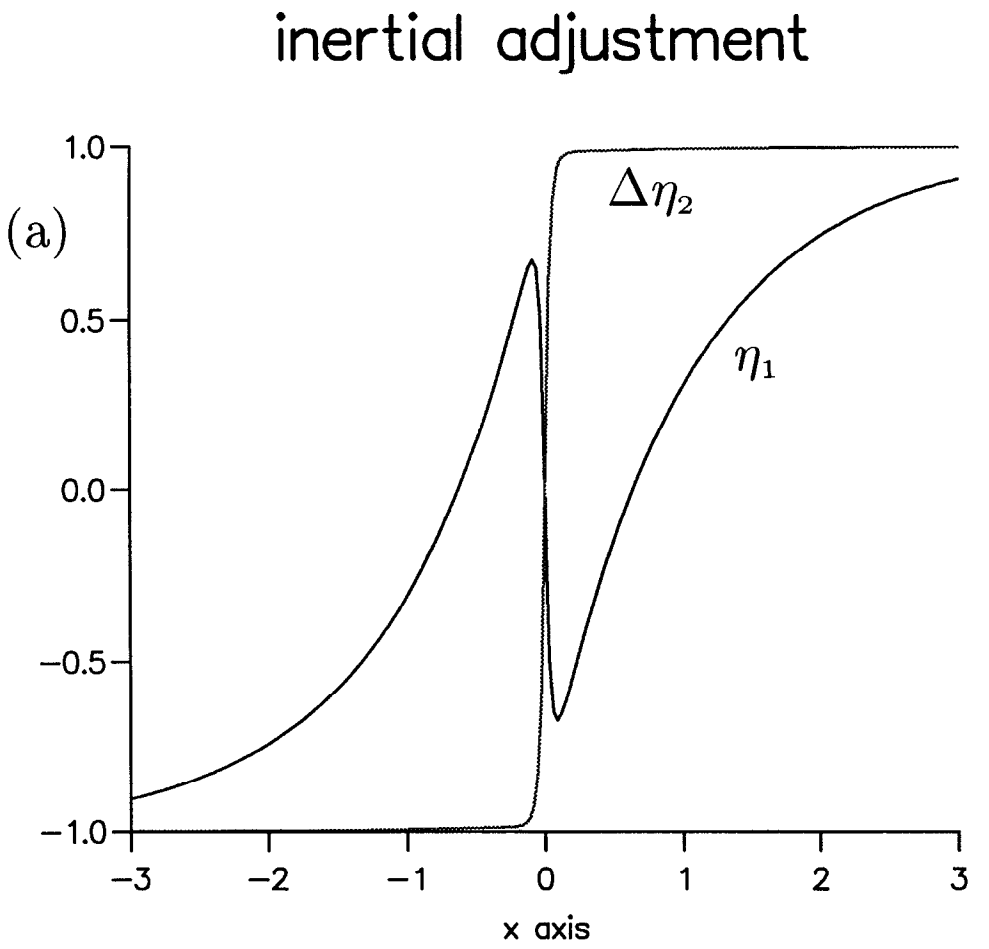

Figure 8. As in Figure 6, except that the initial conditions are $\eta_1 = \Delta\eta_2 = \text{sgn}\,(x)$. Also plotted in (b) is the curve $\eta_1 + \Delta\eta_2$.

velocity field is observed in this study for the case when $\eta_1 = 0$ and $\Delta\eta_2 = \text{sgn}\,(x)$ at $t = 0$. In Figure 7(a) a jet of characteristic width r_i crosses the step in the upper layer, from $y > 0$ to $y < 0$. Directly below the jet, and away from the step, the lower layer flow is in the opposite direction (Fig. 7(c)). Closer to the step the lower layer flow is diverted parallel to it. To date, no analytical studies on the experiments described as Gill *et al.* (1986) have been carried out.

For finite amplitude escarpments the two time scales are not well separated. Further, vertical accelerations will be important in the neighborhood of the escarpment and both these factors conspire to make the Rossby adjustment problem difficult to solve analytically. Nevertheless the key feature of the steady solution

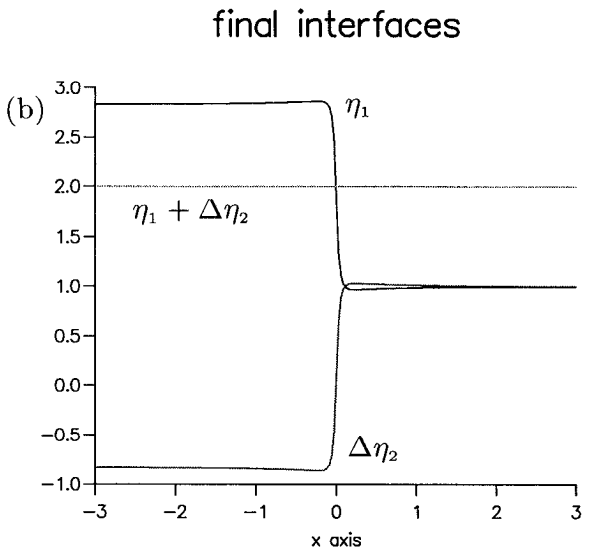

Figure 8. (Continued)

discussed here are expected to hold for the finite amplitude step, namely, non-zero cross-step upper layer flow provided the step is contained entirely in the lower layer.

If an inviscid continuously stratified fluid is viewed as an N-layer fluid, with uniform density ρ_N in layer N with $N \to \infty$, then the results of this study suggest that topography will not block the fluid. This statement is based on the fact that except in the layers which contain the topography, cross-escarpment flow occurs in the steady solution of the Rossby adjustment problem.

Dissipation in the form of interfacial or bottom friction will lead to cross-escarpment flow within frictional boundary layers. However, viscous problems of this type have yet to be solved analytically. Numerical calculations (Allen, 1988 and Wajsowicz, 1991) show the importance of frictional boundary layers in the neighborhood of topography. Process studies of the type reported here help to shed light on how deep water formed in the Arctic basin crosses the Icelandic Ridge to enter the deep North Atlantic basin. Wajsowicz (1991) carried out numerical experiments with a two-year model to address this question. Wajsowicz considers two rectangular ocean basins which are separated by a zonally aligned top hat ridge, the width of which is much greater than the internal Rossby radius of deformation. The numerical calculations show that cross-ridge transport in the lower layer only occurs in boundary layers located where the ridge meets the meridional channel walls. The analysis in this study would predict that without coastal walls perpendicular to the ridge, no cross-ridge transport would occur in the lower layer, unless diffusive effects were extremely large.

Hermann *et al.* (1989) consider nonlinear effects on the inviscid Rossby adjustment

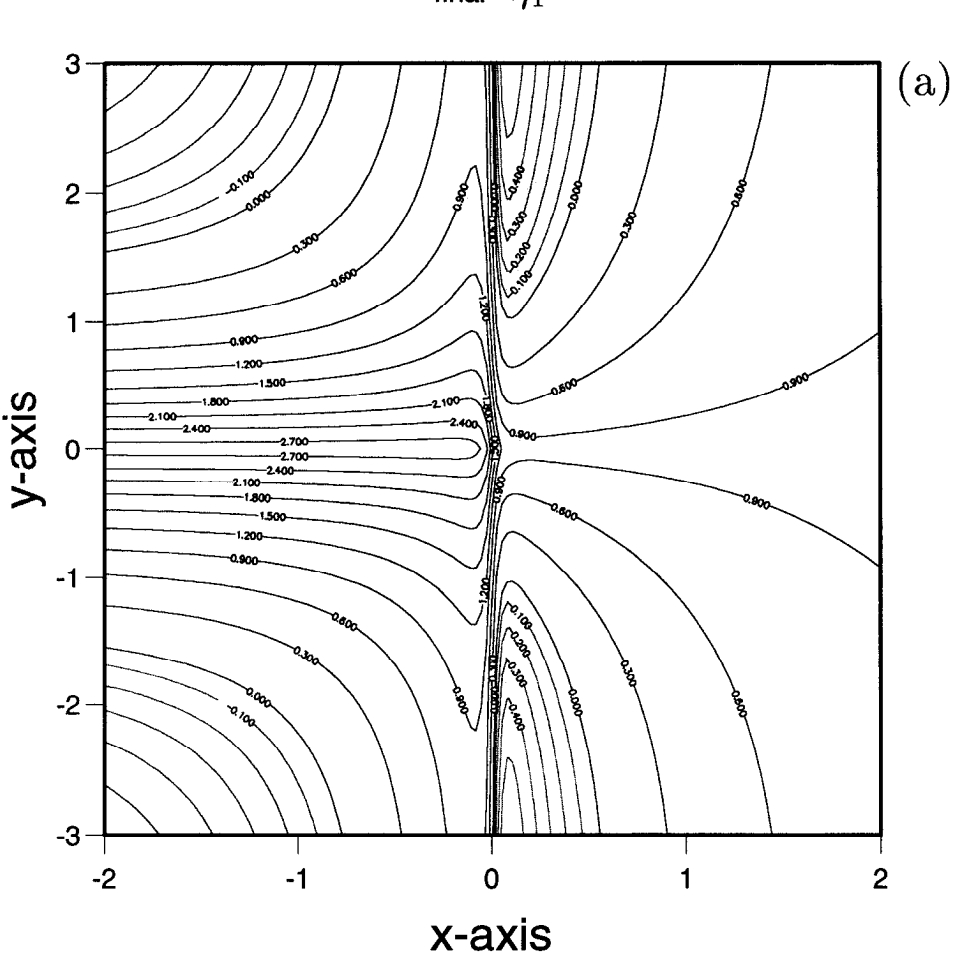

Figure 9. Contour plots of (a) the upper layer streamfunction for the final steady state, η_1; (b) the lower layer streamfunction in the final steady state, $\eta_1 + \Delta\eta_2$. The initial conditions are $\eta_1 = \Delta\eta_2 = \text{sgn}(x)$. In (a), the evenly spaced contour increment is 0.3, and in (b) it is 0.2.

problem for a homogeneous fluid in a channel. The cross-channel barrier that initially separates fluid of different depths forms a potential vorticity front. Nonlinearity leads to the front being advected downstream, leaving behind a symmetric steady flow in the channel. In comparison, linear theory predicts that after the passage of Kelvin waves trapped against the channel walls, an asymmetric steady flow is established. Weak nonlinear effects prevent the linear solution from being valid for all time. Clearly it will be worthwhile to consider the two-layer analogue of the problem addressed by Hermann *et al.* (1989).

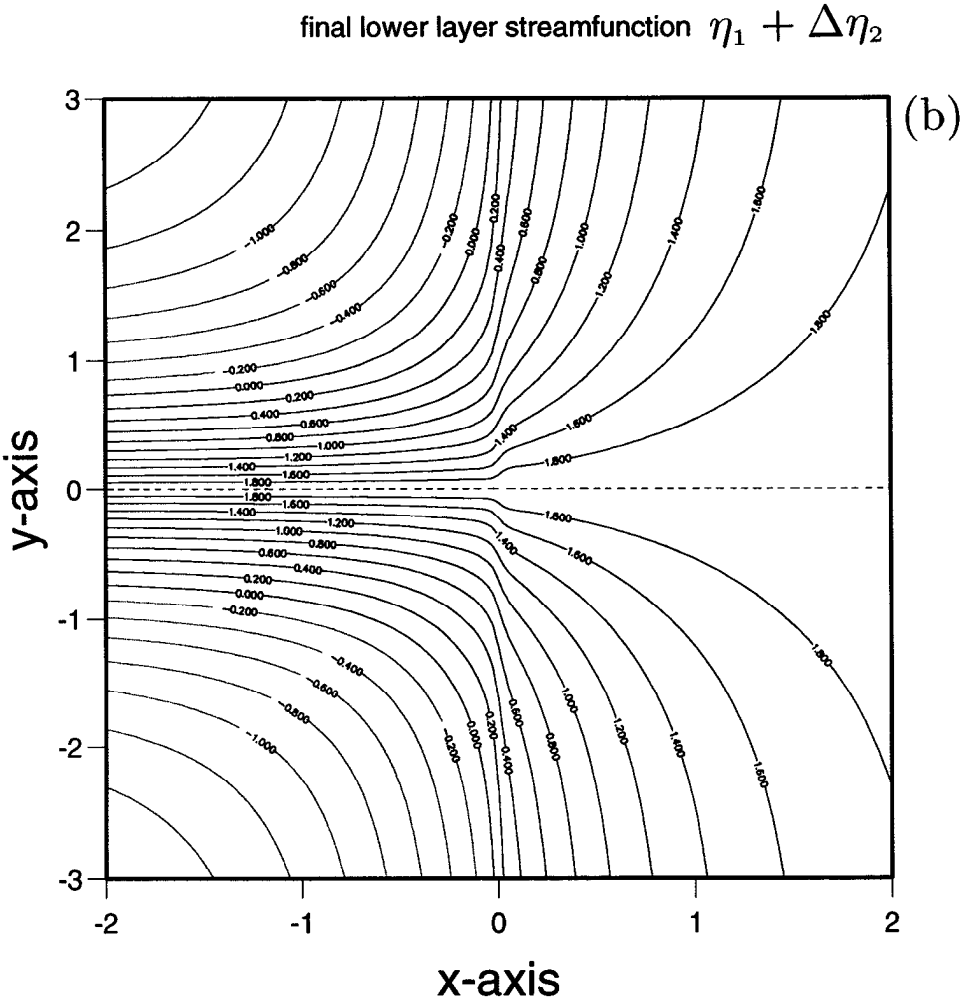

Figure 9. (Continued)

Acknowledgments. AJW is grateful to Ms P. Jones for computing support provided by research grant GR3/8578 from the U.K. Natural Environment Research Council.

APPENDIX A

Evaluation of the Fourier integrals

Consider the Fourier integral

$$I(x, t) = \frac{1}{2\pi} \int_{-\infty}^{\infty} \frac{\hat{F}(k)}{ik} \exp\,[ikx + i\omega(k)t]dk, \tag{A1}$$

where the amplitude $\hat{F}(k)$ and the frequency $\omega(k)$ are real even and odd functions of

k respectively, $\hat{F}(0)$ is finite and the phase speed

$$c_p(k) = \omega(k)/k,$$

is finite for long waves i.e.

$$c_p(0) = c_g(0) = c \text{ (say)},$$

where $c_g(0)$ is the group speed for long waves. Over the escarpment ($y = 0$) the contribution from the time dependent terms in (3.12) can be written in the form (A1). It is convenient to decompose I into the sum of two integrals of the form

$$I_1(x, t) = \frac{1}{2\pi}\int_{-\infty}^{\infty} \frac{\hat{F}(k)}{ik}\{\exp(ikx + i\omega t) - \exp(ikx + ikct)\}dk,$$

$$I_2(x, t) = \frac{1}{2\pi}\int_{-\infty}^{\infty} \frac{\hat{F}(k)}{ik}\exp(ikx + ikct)dk.$$

Now I_1 can be written as

$$\begin{aligned} I_1(x, t) &= \frac{1}{\pi}\int_0^{\infty} \frac{\hat{F}(k)}{k}\{\sin(kx + \omega t) - \sin[k(x + ct)]\}dk \\ &= \frac{2}{\pi}\int_0^{\infty} \frac{\hat{F}(k)}{k}\sin\left[\frac{1}{2}kt(c_p - c)\right]\left\{-\sin kx \sin\left[\frac{1}{2}kt(c_p + c)\right]\right. \\ &\quad \left. + \cos kx \cos\left[\frac{1}{2}kt(c_p + c)\right]\right\}dk, \end{aligned}$$

and therefore the integrand is $O(k)$ as $k \to 0$. Thus

$$\lim_{t\to\infty} I_1(x, t) = 0.$$

Integral I_2 can be written as

$$I_2(x, t) = \frac{1}{\pi}\int_0^{\infty}\left[\frac{\hat{F}(k) - \hat{F}(0)}{k}\right]\sin[k(x + ct)]dk + \frac{1}{2}\hat{F}(0)\,\mathrm{sgn}(x + ct). \quad \text{(A2)}$$

The integral on the right-hand side of (A2) is a function of $x + ct$ only and is well-defined at $k = 0$. In fact for the evaluation of the Fourier integrals (3.12), the forms of $\hat{F}(k)$ are such that, $d\hat{F}(0)/dk = 0$, and therefore

$$\lim_{t\to\infty} I_2(x, t) = \frac{1}{2}\hat{F}(0).$$

APPENDIX B

Parameter values

$H_1 = 450$ m, $H^- = 4500$ m, $\delta = 0.1$ (giving a step height $\delta H^- = 450$ m), $\Delta = 10^{-2}$ (strongly stratified).

REFERENCES

Allen, S. 1988. Rossby adjustment over a slope, PhD thesis, University of Cambridge, 206 pp.

Anderson, D. L. T. and A. E. Gill. 1975. Spin-up of a stratified ocean, with application to upwelling. Deep-Sea. Res., *22,* 583–596.

Gill, A. E., M. K. Davey, E. R. Johnson and P. F. Linden. 1986. Rossby adjustment over a step. J. Mar. Res., *44,* 713–738.

Hermann, A. J., P. B. Rhines and E. R. Johnson. 1989. Nonlinear Rossby adjustment in a channel: beyond Kelvin waves. J. Fluid Mech., *205,* 469–502.

Johnson, E. R. 1984. Starting flow for an obstacle moving transversely in a rapidly rotating fluid. J. Fluid Mech., *149,* 71–88.

—— 1985. Topographic waves and the evolution of coastal currents. J. Fluid Mech., *160,* 499–509.

—— 1990. The low-frequency scattering of Kelvin waves by stepped topography. J. Fluid Mech., *215,* 23–44.

—— 1993. Low-frequency scattering of Kelvin waves by continuous topography. J. Fluid Mech., *248,* 173–201.

Johnson, E. R. and M. K. Davey. 1990. Free surface adjustment and topographic waves in coastal currents. J. Fluid Mech., *219,* 273–289.

Killworth, P. D. 1989. How much of a baroclinic coastal Kelvin wave gets over a ridge? J. Phys. Oceanogr., *19,* 321–341.

Rhines, P. B. 1977. The dynamics of unsteady currents, *in* The Sea, E. D. Goldberg *et al.,* eds., 6, Wiley (Interscience), New York, 189–318.

Wajsowicz, R. C. 1991. On stratified flow over a ridge intersecting coastlines. J. Phys. Oceanogr., 1407–1437.

Willmott, A. J. 1984. Forced double Kelvin waves in a stratified ocean. J. Mar. Res., *42,* 319–358.

Willmott, A. J. and R. H. J. Grimshaw. 1991. The evolution of a coastal current over a wedge shaped escarpment. Geophys. Astrophys. Fluid Dyn., *57,* 19–48.

—— 1992. Reply to comments on "The evolution of a coastal current over a wedge shaped escarpment." Geophys. Astrophys. Fluid Dyn., *65,* 251–253.

Willmott, A. J. and E. R. Johnson 1989. Topographic waves in a rotating stratified basin. Geophys. Astrophys. Fluid Dyn., *45,* 71–87.

Willmott, A. J. and J. A. Johnson. 1979. The effects of horizontal momentum exchange on the spin-up of a stratified ocean. Deep-Sea Res., *26,* 1247–1266.

Received: *12 April, 1994,* revised: *14 July, 1994.*